

# Climatology and Variability of the Ionosphere: Incoherent Scatter Radar Observations

Shun-Rong Zhang and John M. Holt

*Haystack Observatory, Massachusetts Institute of Technology, Westford, Massachusetts*

**Abstract.** Ionospheric climatology and variability studies are conducted using long-term incoherent scatter radar (ISR) observations from seven sites around the world. These studies result in an empirical model system, the ISR Ionospheric Model (ISRIM), which represents local and regional ionospheric climatology and variability of the ionosphere. This paper presents some results of the ISR-based climatology and variability. It is indicated that ionospheric variability changes with height significantly, being large in the F region and small in the E region and in the topside. These changes are dependent of locations. At high latitudes, variability in Ne and Ti in the E region is obviously larger than at midlatitudes and the corresponding percentage variability may become comparable with that in the F region. It is also indicated that in the seasonal variation of the F region electron density variability, the percentage variability is smaller in summer (later summer) than in winter and spring; in the diurnal variation, it is smaller during the day than during the night. Variability is also dependent of the solar flux level. A high F10.7 corresponds to the enhanced variability in summer; the sunrise induced variability is also enhanced.

**Keywords:** Ionosphere, Climatology, Variability, Incoherent Scatter Radar, Modeling

**PACS:** 94

## INTRODUCTION

Studies of the ionospheric climatology and variability have been pursued by many prior workers. It is noted that most prior studies are based on F2 peak parameters, the E peak density and TEC. As one of the most powerful ground-based instruments for probing the Earth's upper atmosphere, an incoherent scatter radar (ISR) directly measures the ionospheric electron density Ne, electron and ion temperatures Te and Ti, and line-of-sight ion velocity over a broad height range. Since the development of ISRs in the 1960's, long-term observational data sets have been accumulating for various ISR sites around the world. Long-term ISR observations provide an extremely valuable data source for addressing significant aspects of ionospheric climatology and variability. The advantage of using such data lies in the broad height range afforded by the radar and the variety of parameters it produces, facilitating synthetic investigations of the relevant ionospheric processes.

The main purpose of our research is to characterize both the climatology and variability of the ionosphere for multiple parameters based on data from multiple ISRs. Our efforts have resulted in an ISR model system, the Incoherent Scatter Radar Model (ISRIM). This system, evolved from that described in [4] and [14], can describe the ionospheric climatology and variability for Ne, Te and Ti for each of the above-mentioned ISR sites with long-term datasets available, as well as for ion velocity for some of those sites. It provides various changes of the local ionosphere as well as of the regional ionosphere, especially, the subauroral/auroral ionosphere.

Results presented here focus more on height variations of ionospheric parameters in the 100-600 km height range, which are yet to be well defined. We will pay more attention to variability, and climatological results are used for comparisons with variability results. The ISR based ionospheric climatology has been reported by [4] for variations at Millstone Hill, [12] and [17] for mid-latitude plasma temperatures, [14] and [13] for climatology over a network of world ISRs, and [16] for high latitude convection climatology.

The day-to-day ionospheric variability, i.e., the off-median behavior, is persistent and significant. This median is often the climatological value. The variability arises primarily from solar flux variability and magnetic activity, with possible contributions from the lower atmosphere. Thermospheric and ionospheric responses to solar flux changes are complicated, depending on height, time of the day, season and geographic location. This complexity carries significant information about the solar impact on the earth's upper atmosphere, including its intrinsic chemistry and dynamics. It can occur on hourly, daily, seasonally, and solar cycle scales. In particular, during quiet magnetic conditions, the day-to-day variability or the variability on a temporal scale much less than monthly and seasonally is considered to be related with activity in the lower atmosphere, including acoustic, tidal, and planetary waves, as well as meteorological processes. See [3], [2], [11], [1], [6], [5], [10] for some of recent publications.

In this paper, we will first describe the technique of processing the ISR long-term datasets for characterizing the ionospheric climatology as part of ISRIM, which is

the base for variability studies. The technique used to represent the local ionospheric variability in the ISRIM system will be also discussed. In the result section, we will present profiles of variability from different locations, and the time variation of the F region electron density variability as well. We will also discuss effects of solar flux variability.

## CHARACTERIZING CLIMATOLOGY AND VARIABILITY: ISRIM

The ISRIM comes from a system that dealt with Millstone Hill incoherent scatter radar local and regional observations collected using the radar's 68 m zenith antenna and 46 m steerable antenna. The ISRIM consists of models for the ionospheric climatology and variability. It provides local models of Ne, Te and Ti for each of the following ISR sites: Svalbard (78.1°N, 16.0°E; geodetic coordinates, the same hereafter), Sondrestrom (67.0°N, 309.0°E), Tromsø (69.6°N, 19.2°E), Millstone Hill (42.6°N, 288.5°E), St. Santin (44.6°N, 2.2°E), Arecibo (18.3°N, 293.2°E), and Shigaraki (34.8°N, 136.1°E). ISRIM was fully described in an appendix by [13]. The brief description given below highlights some of the key features.

### ISRIM local climatology

The ISR data are binned by month and local time with 3-month and 1-hour bin sizes. In this initial step of data binning, we assume a linear variation between any two consecutive altitude nodes (i.e., piecewise-linear variation over the entire height range), and the constant and linear coefficient in the linear equation for each height segment can be calculated. Each constant and linear coefficient is further assumed to be linear in the solar activity index F107 and magnetic activity index 3-hourly ap. A sequential least squares fit to the solar and magnetic activity dependence and to the piecewise-linear function for altitude dependence is then performed, generating coefficients for the constant, F107 and ap terms. Here F107 is an average between the daily F107 index and the 81-day running average of the daily F107 centering at the current day (see [9]). The initial binning results are then represented by a 3-D basis with a cubic B-spline function to give twice-differentiable height variations, and harmonics with 12-, 6- and 4- month periodicities for seasonal changes and with 24-, 12-, 8-, and 6-hour periodicities for local time changes. This process is applied to Ne, Te and Ti for each ISR site, and results in local climatological models of the ISRIM.

It is noted that in the earlier step of data binning, using the piecewise-linear function has some advantages over using simply averaging for binning. The piecewise-linear function approach leads to better determined bin/node values by considering contributions from the neighboring points weighted by the distance from the node. If we were using a simpler approach of averaging over an altitude bin, for instance, height variations within a bin would be neglected.

### ISRIM local variability

Our evaluation of the ionospheric variability is based on the difference (residual) between individual measurements and the corresponding climatological average. The average is provided by the ISRIM climatology, and the measurements are those used for constructing the ISRIM climatology. To drive the ISRIM climatology, F107p, ap, day number of the year, local solar mean time and geodetic height corresponding to the measurement data are used. The difference is squared and goes into the same modeling system as used to produce the ISRIM climatology, i.e., 1) bin data according to local time and month, 2) represent the height variation by a piecewise-linear function, and represent the solar and magnetic dependence using a linear function with F107p and ap terms, i.e.,

$$\mathfrak{R}^2 = \delta_b^2 + c_1 \times f + c_2 \times a \quad (1)$$

where  $f$  is the normalized F107p and  $a$  the normalized ap, and  $c_1$  and  $c_2$  are linear constants), and 3) after the initial step of least squares fitting the linear coefficients, finally express the bin/node coefficients using a 3-D basis function with cubic B-splines and harmonics such that Equation (1) becomes

$$\sigma^2 = \sigma_b^2 + k_1 \times f + k_2 \times a \quad (2).$$

Therefore, the ISRIM variability is coherent with ISRIM climatology in terms of the data source and technique used for handling the data; the ISRIM climatology deals with a specific physical parameter, while the ISRIM variability deals with the mean squared difference of a physical parameter from its climatology value. Our results to be discussed include the (absolute) variability,  $\sigma$ , defined as the square root of the mean squared difference values and the relative or percentage variability defined as the absolute variability divided by the climatology value.

### ISRIM data resources

All ISR data were obtained from the Madrigal database (<http://www.openmadrigal.org>)

developed at MIT Haystack Observatory. Up to December 2004, the number of experiments for Svalbard (operational since 1996) is over 600, for Sondrestrom (operational since 1983) over 1000, for the EISCAT Tromsø (operational since 1981) over 1200 (over 900 for the UHF radar), for Millstone Hill (operational since 1960) over 1000 experiments, for St. Santin (operational during 1963-1987) about 100 experiments, for Shigaraki (operational since 1986) about 200 experiments, and for Arecibo (operational since 1963) over 100 experiments. Each ISR experiment covers typically 3-7 days, though a calibration run can be as short as a few hours during one day. There were also 30 day experiments for some sites. At high latitudes there are relatively fewer data in summer than in other seasons. St. Santin has the fewest data but they are nearly equally distributed with month. Outside the polar and auroral areas there are much more data in the F region than in the E region where the ionosphere is, however, less variable and more easily characterized.

## RESULT AND DISCUSSION

### Height variations

We now discuss results of height profiles for ionospheric climatology and variability from various ISR locations. The plots given in Figures 1-4 are for midday for winter with day number of the year 15, median solar activity conditions with solar F107 index 135, and quiet magnetic activity with  $ap$  15. For Ne as shown in Figures 1 and 2, the absolute variability is always largest at the F2 peak, and it decreases quickly below and above the height. In those three sites given in Figure 1, Svalbard is normally located in dayside cusp, and the relative (percentage) variability (shown as dashed line is normalized to the maximum percentage), is highest among the three sites; Sondrestrom is near the auroral zone and variability is also very high. The midlatitude site St. Santin has a smaller level of variability. The high level of variability at high latitudes is more likely due to complicated magnetosphere-ionosphere-thermosphere interaction, although low magnetic activity conditions are selected. In fact, the relative variability in the E region is as large as or even larger than that in the F2 peak height. This may be caused by variability in the energetic particle-produced ionization.

In Figure 2, the Millstone Hill plot extends to 1000 km while the MU radar (Shigaraki, Japan) plot starts from 200 km. The Arecibo plot displays clearly an F1-layer. Variability in the intermediate layer, the F1-layer, is also at the intermediate level between E and F regions. In general, the relative variability reaches a maximum near

or slightly above the F2 peak, then it decreases gradually with increasing height. In fact the change in the level of variability is little up to about 600 km, and this is largely due to the diffusion effect. If the plasma temperature changes appreciably with height, the diffusion effect can result in height dependency of the variability.

It can be seen, for this particular case of median solar activity and quiet magnetic activity in winter, that near 150 km slightly below the F1-ledge and above the E-F valley, a minimum in the variability exists typically for Svalbard, Sondrestrom, Millstone Hill. This height of minimum variability is lower for St. Santin and higher Arecibo. It is not very clear at this point whether this is what was identified by [8], however, extensive investigations into this feature will be conducted in the future.

Figures 3-4 are plasma temperature results. High latitude sites show much larger variability in the temperatures, indicating stronger energetic processes originating from the solar wind and magnetosphere. In general,  $T_i$  variability at low altitudes in the E region is greater than corresponding  $T_e$  variability, while  $T_e$  variability at high altitudes in the F region is greater than  $T_i$  variability. This is mostly due to various heating processes, corresponding to different energy spectra of precipitating particles, which are height dependent. At midlatitudes,  $T_i$  variability is very weak.

### Time variations

Now we discuss time variations of the electron density (in log10 scale) using results for Millstone Hill as an example. Figure 5 shows a day number verse local time plot at 300 km for median solar activity and quiet magnetic activity conditions. The upper panel shows climatological values. In the annual variation, the midday Ne is high in winter than in summer and the midnight Ne is high in summer than in winter. The semiannual variation is also presented with the highest midday Ne in autumn. For the variability (percentage variability), however, the daytime variability, with a maximum near noon in winter and near prenoon hours in spring, is relatively weaker than the nighttime variability. The stronger nighttime variability indicates the importance of dynamical processes at night, and the weaker daytime variability suggests the photoionization effect which stabilizes the ionospheric variability in Ne. In the seasonal variation, the daytime variability in summer is weaker, and the nighttime variability is weaker in winter.

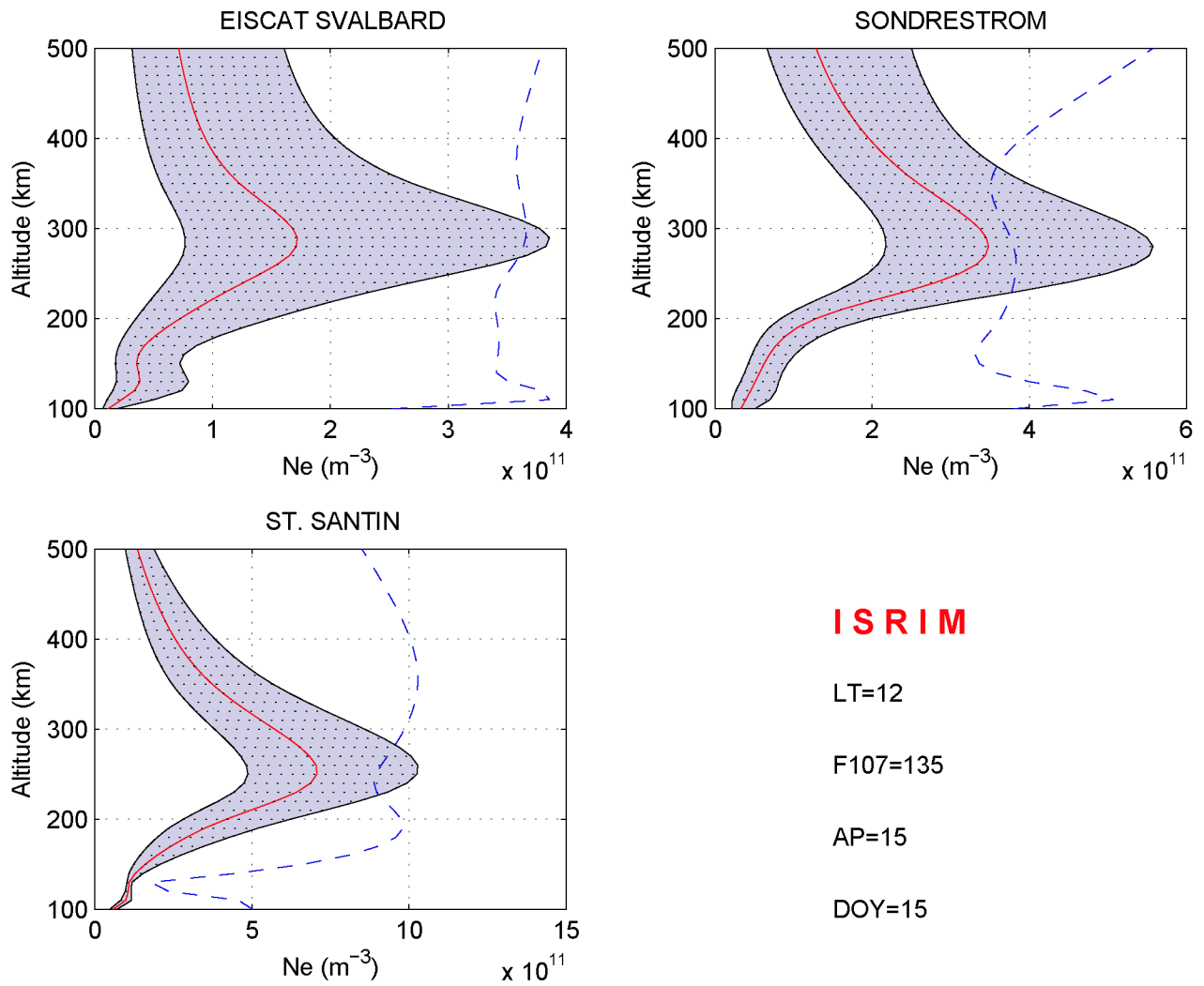


**FIGURE 1.** Noontime profiles of ionospheric Ne climatometry and variability for Svalbard (69.6°N, 19°E), Sondrestrom (67°N, 51°W), and St. Santin (44.6°N, 2.2°E), with day number of the year = 15, F107 = 135, and AP = 15.

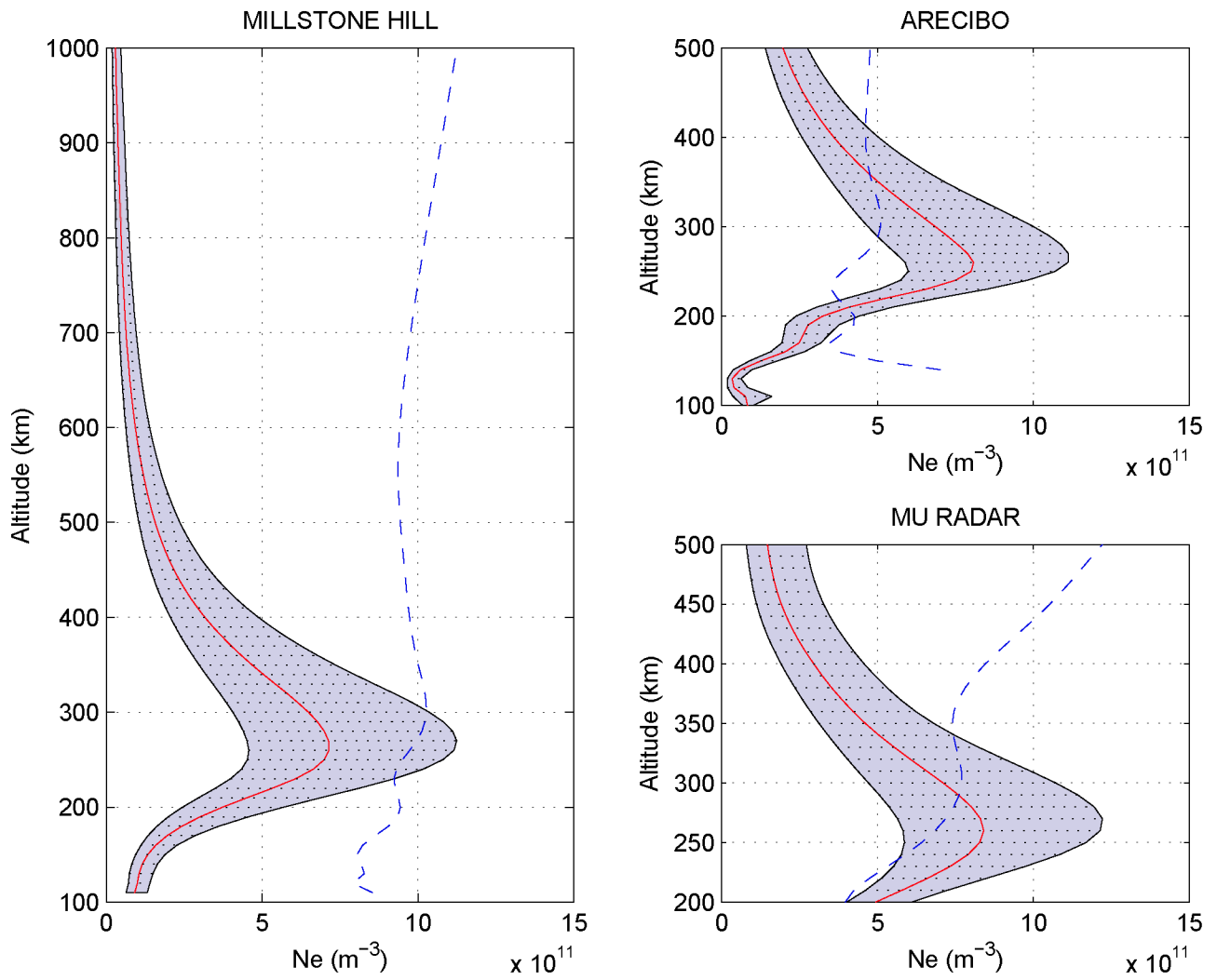


**FIGURE 2.** Noontime profiles of ionospheric Ne climatometry and variability for Millstone Hill (42.6°N, 71.5°W), Arecibo (18.3°N, 66.7°W), and Shigaraki (34.8°N, 136.1°E), with day number of the year = 15, F107 = 135, and AP = 15.

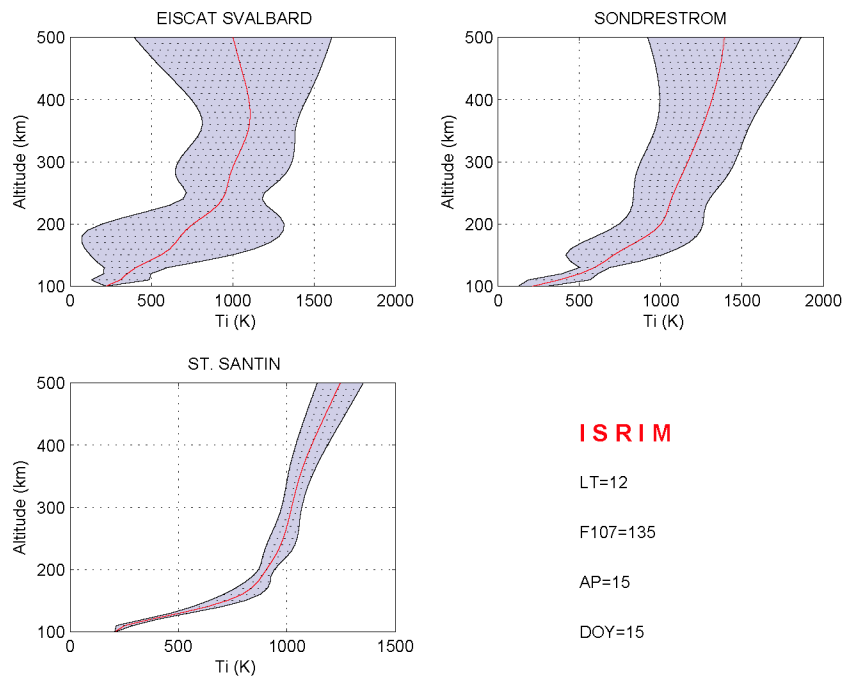


**FIGURE 3.** Noontime profiles of ionospheric  $T_i$  climatology and variability for Svalbard ( $69.6^\circ\text{N}$ ,  $19^\circ\text{E}$ ), Sondrestrom ( $67^\circ\text{N}$ ,  $51^\circ\text{W}$ ), and St. Santin ( $44.6^\circ\text{N}$ ,  $2.2^\circ\text{E}$ ), with day number of the year = 15,  $F_{107} = 135$ , and  $AP = 15$ .

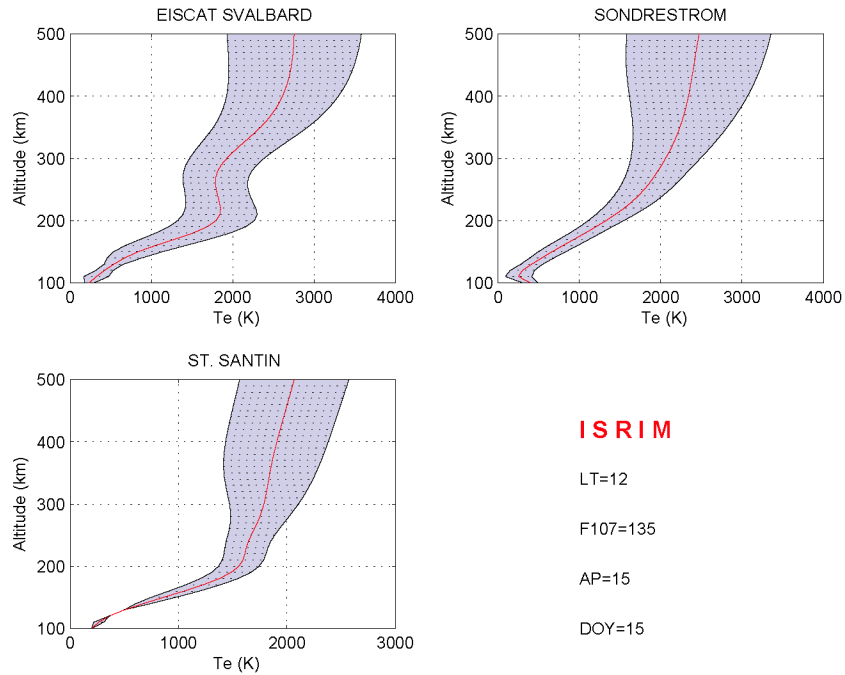


**FIGURE 4.** Noontime profiles of ionospheric  $T_e$  climatology and variability for Svalbard ( $69.6^\circ\text{N}$ ,  $19^\circ\text{E}$ ), Sondrestrom ( $67^\circ\text{N}$ ,  $51^\circ\text{W}$ ), and St. Santin ( $44.6^\circ\text{N}$ ,  $2.2^\circ\text{E}$ ), with day number of the year = 15,  $F_{107} = 135$ , and  $AP = 15$ .

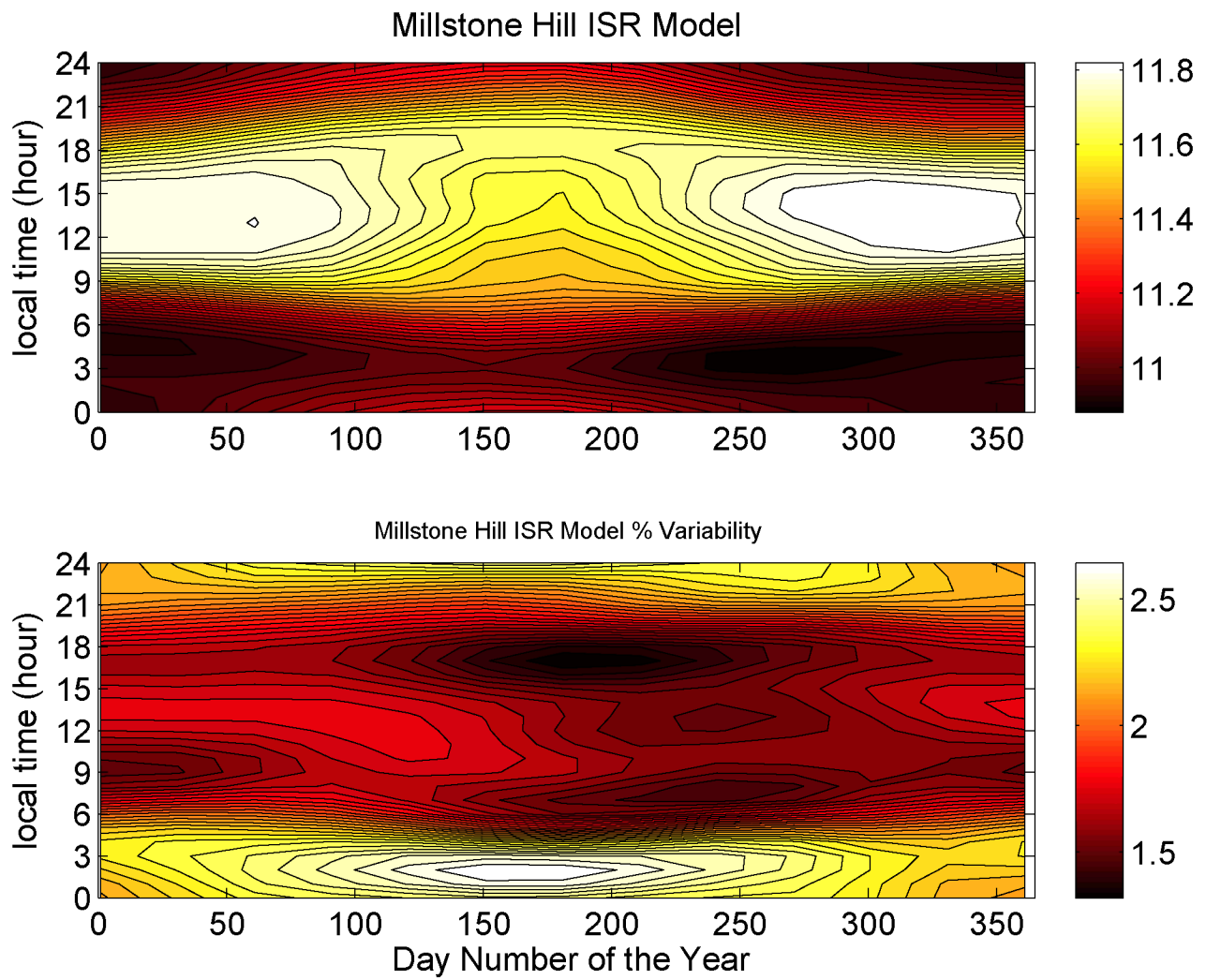


**FIGURE 5.** Climatology (upper panel) and variability (in percentage, bottom panel) of electron density (in log<sub>10</sub> scale) at 300 km for Millstone Hill with F<sub>107</sub> = 135 and AP = 15 as a function of day number and local time.

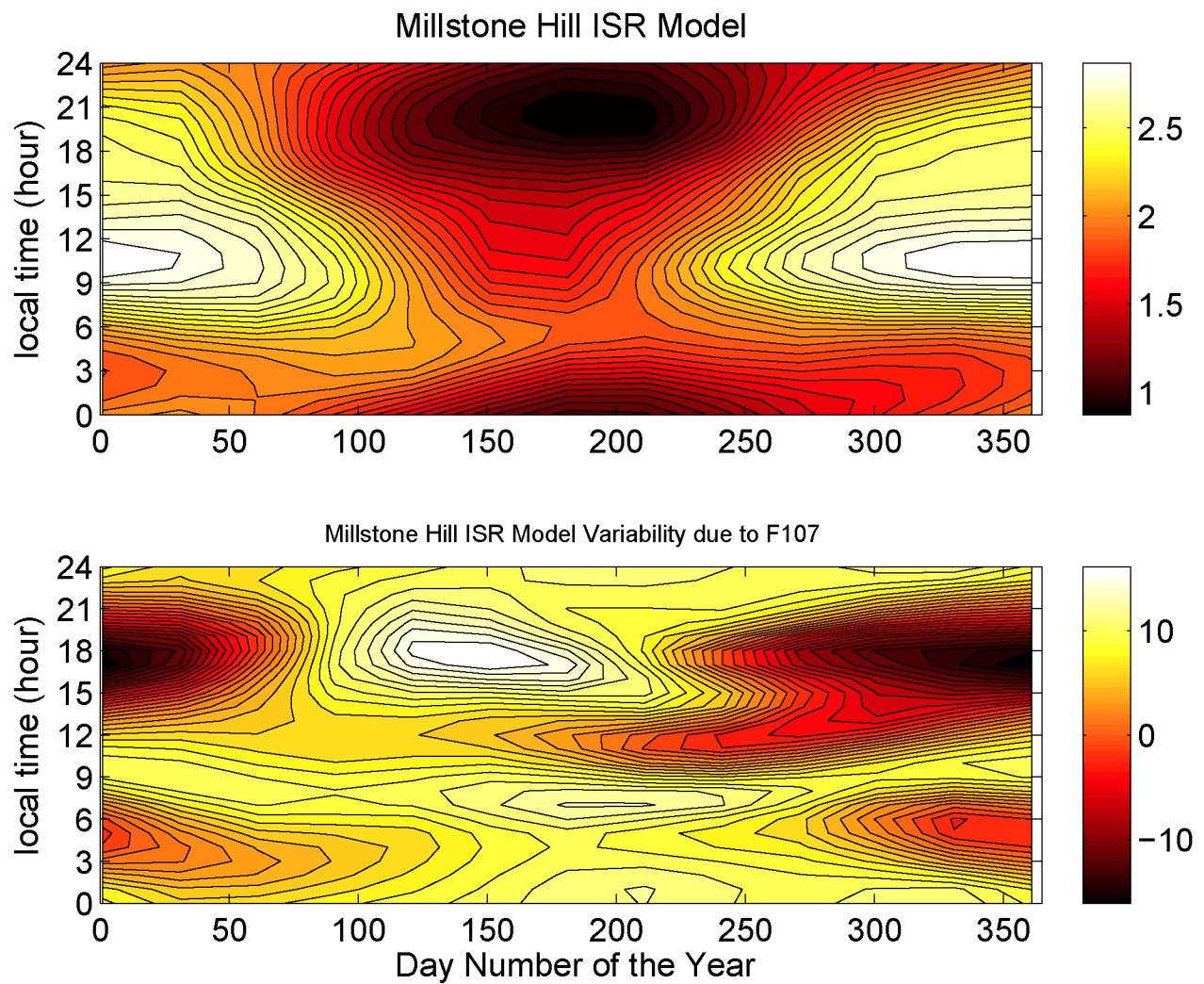


**FIGURE 6.** Effects of solar flux on variability shown for electron density (in log<sub>10</sub> scale) at 300 km for Millstone Hill as a function of day number and local time. Upper panel shows climatological results for the percentage contribution of the solar 10.7 cm flux change by 50 units out of the background, and the bottom shows variability results for the percentage contribution of the solar 10.7 cm flux change by 50 units out of the background (see text)

## Solar activity dependency

Our variability for given height, season and local time, as discussed in Section 2, is expressed as Equation (2) with a background term  $\sigma_b^2$ , a solar flux term and a magnetic activity term. There is a similar equation for climatology variations. We now consider the solar flux term contributions to climatology and variability as a result of F10.7 change by 50 units. These contributions are given as a percentage out of the background value.

The upper panel in Figure 6 shows the climatological result. Obviously Ne increases as F10.7 increases by 50. The Ne increase is more significant in winter and equinox, because of high atomic oxygen over molecules density ratio in these seasons, and it is larger by day when photoionization effects come to play than by night. What is interesting is the result of variability. Variability is reduced as F10.7 increases for evening hours in autumn through winter days. Variability tends to be unchanged in pre-dawn hours in winter. The highest increase appears in evening hours in earlier summer, as well as in the morning hours, being late in winter and earlier in summer. This former enhancement zone shown in the figure is perhaps related to the well-known electron density increase in the evening hours in summer, for which neutral winds are considered to be important. The later zone of high increases in variability is associated with sunrise times.

## SUMMARY

Ionospheric climatology and variability studies are conducted using long-term incoherent scatter radar (ISR) observations from seven sites around the world. These studies result in an empirical model system, the ISR Ionospheric Model (ISRIM), which describes local and regional ionospheric climatology and variability of the ionosphere. We have presented some preliminary results from these models, with an emphasis on ionospheric variability.

It is indicated that ionospheric variability changes with height significantly, being large in the F region and small in the E region and in the topside. These changes are dependent of locations. At high latitudes, variability in Ne and Ti in the E region is obviously larger than at midlatitudes and the corresponding percentage variability may become comparable with that in the F region. It is also indicated that in the seasonal variation of the F region electron density variability, the percentage variability is smaller in summer (later summer) than in winter and spring; in the diurnal variation, it is smaller during the day than during the night. Variability is also dependent of the solar flux level. A high F10.7 corresponds to the enhanced variability in summer; the sunrise induced vari-

ability is also enhanced.

## ACKNOWLEDGMENTS

We thank the staff at EISCAT, Svalbard, Sondrestrom, and in particular, Bill Wrideout and members of the Haystack Observatory Atmospheric Sciences Group for assembling and maintaining the Madrigal Database. We thank S. Kawamura for preparing the MU radar data. This research was supported by NSF Space Weather Grant ATM-0207748. The Sondrestrom, Millstone Hill and Arecibo incoherent scatter radars are supported by the US National Science Foundation. EISCAT is an international association supported by the research councils of Finland (SA), France (CNRS), the Federal Republic of Germany (MPG), Japan (NIPR), Norway (NFR), Sweden (VR) and the United Kingdom (PPARC). The MU radar belongs to and is operated by the Research Institute for Sustainable Humanosphere of Kyoto University. St. Santin and Arecibo data are imported from the CEDAR database.

## REFERENCES

1. D. Altadill and E. M. Apostolov, Vertical propagating signatures of wave-type oscillations (2- and 6.5-days) in the ionosphere obtained from electron-density profiles, *J. Atmos. Sol. Terr. Phys.*, **63**, 823-834 (2001).
2. J. M. Forbes, S. E. Palo, X. Zhang, Variability of the ionosphere, *J. Atmos. Sol. Terr. Phys.*, **62**, 685-693 (2000).
3. J. M. Forbes and X. Zhang, Quasi 2-day oscillation of the ionosphere: a statistical study, *J. Atmos. Sol. Terr. Phys.*, **59**, 1025-1034 (1997).
4. J. M. Holt, S.-R. Zhang and M. J. Buonsanto, Regional and Local Ionospheric Models Based on Millstone Hill Incoherent Scatter Radar Data, *Geophys. Res. Lett.*, **29**, 0.1029/2001GL013579 (2002).
5. J. Laštovička, Forcing of the ionosphere by waves from below, *J. Atmos. Sol. Terr. Phys.*, **68**, 479-497 (2006).
6. M. Mendillo, H. Rishbeth, R. G. Roble, and J. Wroten, Modelling F2-layer seasonal trends and day-to-day variability driven by coupling with the lower atmosphere, *J. Atmos. Sol. Terr. Phys.*, **64**, 1911-1931 (2002).
7. M. Mendillo, J. Baumgardner, J. Aarons, J. Foster, and J. Klobuchar, Coordinated Optical and Radio Studies of Ionospheric Disturbances: Initial Results from Millstone Hill, *Ann. Geophys.*, **5A**, 543-550 (1987).
8. M. Mosert de Gonzalez and S. M. Radicella, Study of ionospheric variability at fixed heights using data from South America, *Adv. Space Res.*, **15(2)**, 61-65 (1995).
9. P. G. Richards, D. G. Torr, B. W. Reinisch, R. R. Gamache, P. J. Wilkinson, F2 peak electron density at Millstone Hill and Hobart: Comparison of theory and measurement at solar maximum, *J. Geophys. Res.*, **99**, 15005-15016, 10.1029/94JA00863 (1994).
10. H. Rishbeth, F-region links with the lower atmosphere?, *J. Atmos. Sol. Terr. Phys.*, **68**, 469-478 (2006).

11. H. Rishbeth, and M. Mendillo, Patterns of F2-layer variability, *J. Atmos. Sol. Terr. Phys.*, **63**, 1661-1680 (2001).
12. S.-R. Zhang and J. M. Holt, Ionospheric plasma temperatures during 1976-2001 over Millstone Hill, *Adv. Space Res.*, **33**, 963-969, DOI 10.1016/j.asr.2003.07.012 (2004).
13. S.-R. Zhang, and J. M. Holt, Ionospheric Climatology and Variability from Long-term and Multiple Incoherent Scatter Radar Observations: Climatology in Eastern American Sector, *J. Geophys. Res.*, **12**, A06328, doi:10.1029/2006JA012206 (2007).
14. S.-R. Zhang, J. M. Holt, A. P. van Eyken, M. McCready, C. Amory-Mazaudier, S. Fukao, and M. Sulzer, Ionospheric local model and climatology from long-term databases of multiple incoherent scatter radars, *Geophys. Res. Lett.*, **32**, L20102, doi:10.1029/2005GL023603 (2005).
15. S.-R. Zhang, J. M. Holt, A. P. van Eyken, M. McCready, C. Amory-Mazaudier, S. Fukao, and M. Sulzer, Multiple-site comparisons between models of incoherent scatter radar and IRI, *Adv. Space Res.*, **39**, 910-917, doi:10.1016/j.asr.2006.05.027 (2007).
16. S.-R. Zhang, J. M. Holt, and M. McCready, High latitude convection based on long-term incoherent scatter radar observations in North America, *J. Atmos. Sol. Terr. Phys.*, **69**, 1273-1291, doi:10.1016/j.jastp.2006.08.017 (2007).
17. S.-R. Zhang, J. M. Holt, A. M. Zalucha, and C. Amory-Mazaudier, Mid-latitude ionospheric plasma temperature climatology and empirical model based on Saint Santin incoherent scatter radar data from 1966-1987, *J. Geophys. Res.*, **109**, A11311, doi:10.1029/2004JA010709 (2004).